Gas and Vapor Sorption and Permeation in Poly(2,2,4-trifluoro-5-trifluoromethoxy-1,3-dioxole-*co*-tetrafluoroethylene)

Rajeev S. Prabhakar,[†] Benny D. Freeman,*[,†] and Ian Roman[‡]

Department of Chemical Engineering, The University of Texas at Austin, Austin, Texas 78758, and MEDAL L.P., Newport, Delaware 19804

Received June 2, 2004; Revised Manuscript Received July 26, 2004

ABSTRACT: The solubilities of N_2, CO_2, CH_4, C_2H_6, C_3H_8, and C_3F_8 and permeabilities of N_2, O_2, CO_2, CH_4, C_2H_6, and C_3H_8 were determined in a glassy, amorphous fluoropolymer prepared from 80 mol % 2,2,4-trifluoro-5-trifluoromethoxy-1,3-dioxole (TTD) and 20 mol % tetrafluoroethylene (TFE), commercially known as Hyflon AD 80. This polymer exhibits lower increases in hydrocarbon gas and vapor solubility with increasing penetrant critical temperature than conventional hydrocarbon polymers. On the basis of a best fit of the natural logarithm of solubility vs critical temperature, Hyflon AD 80 should have much lower solubility for high molar mass hydrocarbon compounds (e.g., *n*-decane) than conventional hydrocarbon polymers. Pure gas CO_2/CH_4 separation properties of this polymer are comparable with those of some hydrocarbon polymers considered for natural gas purification. When exposed to a feed stream containing a mixture of CO_2 and CH_4, the polymer exhibits a CO_2 permeability of approximately 250 barrers and a CO_2/CH_4 mixed-gas selectivity of 10.6 at 1.6 atm CO_2 partial pressure. The mixed gas selectivity decreases minimally as CO_2 partial pressure increases to 10.6 atm. The mixed gas selectivity is also maintained when moderate amounts of toluene and *n*-hexane are present in the CO_2-CH_4 feed stream. Diffusion coefficients, calculated from pure gas permeability and solubility coefficients, suggest membrane plasticization at higher pressures of CO_2 and C_2H_6. The polymer also exhibits reversible hysteresis in C_3H_8 permeability with pressure.

Introduction

Polymer membrane-based CO_2 removal from natural gas is gaining attention due to the compact size, low-energy requirement, ease of use and scale-up, and potential for offshore installation of membrane systems.[1] CO_2 is smaller and has a higher critical temperature than CH_4,[2] so both diffusivity and solubility favor CO_2 transport over CH_4 in polymers. Most materials science research in this area has concentrated on backbone modification of hydrocarbon-based polymers to increase gas diffusion coefficients and diffusivity selectivity, thereby achieving higher CO_2 permeability and CO_2/CH_4 selectivity simultaneously.[3] These efforts have produced high-performance materials like aromatic polyimides which now compete with cellulose acetate, a polymer widely used in this application.[4]

Natural gas typically contains a wide variety of aliphatic and aromatic hydrocarbon compounds.[5] These hydrocarbons usually have high solubilities in hydrocarbon-based polymers.[6] Thus, despite being present in small amounts in natural gas (even after pretreatment of the feed gas to remove them), such components still sorb into polymers in significant amounts.[7] The sorption of considerable amounts of CO_2 and/or large aliphatic and aromatic hydrocarbon compounds plasticizes hydrocarbon-based polymer membranes, thereby reducing the diffusivity selectivity that is largely responsible for their high CO_2/CH_4 selectivity. For example, CO_2/CH_4 selectivity of an aromatic polyimide (6FDA−mPD) decreases from 58 under pure gas conditions to approximately 4 in a 50:50 gas mixture at about 17.5 atm total pressure.[8] White et al. report that the CO_2/CH_4 selectivity of another aromatic polyimide (6FDA−DMB) decreases from 33 in pure gas measurements (20.4 atm of CH_4, 6.8 atm of CO_2, 22 °C) to 19 in mixed gas measurements (10% CO_2 in CH_4, 68 atm total pressure, 22 °C).[9] The mixed gas CO_2/CH_4 selectivity (14.6 at 48 °C) decreases to less than 10 when the CO_2-CH_4 feed gas stream is saturated with higher hydrocarbons like toluene or *n*-hexane.[9] Loss in CO_2/CH_4 selectivity results in a loss of the product, methane, from the feed stream into the low-pressure permeate stream. This requires either a second membrane module to recover the lost product and recompress it to pipeline specifications or simply accepting the loss; both are expensive, inefficient options.

Efforts have been made to suppress plasticization of hydrocarbon polymers by blending with other polymers,[10,11] thermal treatment,[12] and cross-linking.[8,13,14] While some success has been achieved in delaying the onset of plasticization to higher penetrant partial pressures, these approaches treat the symptom rather than the fundamental cause of the plasticization phenomenon. An alternative approach is to address the central issue of high solubility of higher hydrocarbon compounds in conventional membrane materials by considering polymeric materials with inherently low solubility for these compounds. Such materials might be more resistant to plasticization by higher hydrocarbons.

Gas solubility in liquids and polymers generally increases with gas condensability (as measured by critical temperature, normal boiling point, or Lennard-Jones force constant) in the absence of specific interactions between the gas and the solvent medium.[15] Unfavorable interactions between the penetrant and the matrix into which the penetrant is dissolving can suppress gas solubility below that expected on the basis of this general correlation. For example, Michaels and Bixler report that the solubility of sulfur hexafluoride

[†] The University of Texas at Austin.
[‡] MEDAL L.P.
* Corresponding author: e-mail freeman@che.utexas.edu; phone (512) 232-2803; Fax (512) 232-2807.

10.1021/ma048909f CCC: $27.50
Published on Web 09/11/2004

Table 1. Ratio of Propane to Nitrogen Solubility Coefficients in Hydrocarbon and Fluorocarbon Media

classification	medium	fractional free vol[a]	solubility selectivity C_3H_8/N_2
hydrocarbons	*n*-C_7H_{16}[46]	0.31	99[c]
	poly(1-trimethylsilyl-1-propyne)[53]	0.29	64[d]
	c-C_6H_{12}[22]	0.28	130[c]
	C_6H_6[22]	0.27	89[c]
	polyethylene[16]	0.22[b]	96[e]
	natural rubber[16]	0.22[b]	89[e]
	poly(butadiene)-hydrogenated[16]	0.19[b]	83[e]
	poly(dimethylsiloxane)[17]	0.16	68[f]
fluorocarbons	AF2400[28]	0.33	22[f]
	n-C_7F_{16}[46]	0.31	18.5[c]
	AF1600[28]	0.30	15[f]

[a] Calculated using Bondi's group contribution method.[31] [b] Calculated using an amorphous phase specific volume of 1.171 cm^3/g.[16] [c] 1 atm and 25 °C. [d] Infinite dilution and 35 °C. [e] For completely amorphous polymer at 25 °C. [f] Infinite dilution and 25 °C.

in low-density polyethylene (LDPE) and natural rubber is 3−4 times lower than expected on the basis of their correlation between solubility and Lennard-Jones force constant.[16] Kamiya et al. observed similar behavior for SF_6 solubility in poly(dimethylsiloxane) (PDMS).[17] Perfluorinated gases like CF_4, C_2F_6, and C_3F_8 also exhibit much lower solubility in hydrocarbon-based polymers like PDMS[18] and LDPE[17] than expected on the basis of a linear relationship of the logarithm of solubility of light gases (N_2, O_2) and hydrocarbons with gas critical temperature. This low solubility of perfluorocarbon gases in hydrocarbon-based polymers has been attributed to unfavorable interactions between perfluorocarbons and hydrocarbons.[19] Such interactions also reduce hydrocarbon solubility in fluoropolymers.[18] For example, Table 1 compares the ratio of propane to nitrogen solubility in several hydrocarbon-rich media with that in a perfluorinated liquid and two fluoropolymers. Propane solubility is approximately 65−130 times larger than nitrogen solubility in the hydrocarbon liquids and polymers. In stark contrast, in the perfluorinated liquid and the high-free-volume, glassy fluoropolymers, AF2400 (fractional free volume, FFV = 0.33) and AF1600 (FFV = 0.30), propane solubility is only about 15−20 times higher than nitrogen solubility. Since nitrogen is not expected to experience specific interactions with these media, the significant reduction in propane to nitrogen solubility ratio results from dramatically lower than expected propane solubility in the perfluorinated media. To the extent that penetrant concentration in the polymer influences the degree of plasticization, lower hydrocarbon solubility may result in greater resistance of fluoropolymers to plasticization by hydrocarbon compounds, making them more attractive as membrane materials for separating gas streams containing these hydrocarbon penetrants.[20,21]

Unexpectedly low solubilities of gaseous hydrocarbons in liquid fluorocarbons and gaseous fluorocarbons in hydrocarbon liquids have been observed previously, and these results attracted considerable interest because the depression in solubility could not be explained by regular solution theory.[22,23] Geometric mean rules for estimating fluorocarbon−hydrocarbon interactions upon mixing appear to systematically overestimate the energy of interaction between unlike molecules. In 1958, after considerable work in this area, Scott surveyed the explanations advanced in the literature to describe this effect and suggested that the two ideas having the greatest promise to rationalize this anomalous behavior were the following: (1) the ionization potentials of hydrocarbons and fluorocarbons are sufficiently different that the assumption of similar ionization potentials between unlike molecules, which underpins the geometric mean approximation, is violated, and (2) the assumption of a spherically symmetric force field about molecules is not appropriate for fluorocarbons.[24] The large electronegativity of fluorine localizes the electrons closer to the fluorine atoms, thus distorting electronic symmetry about the central atom and introducing effects of molecular orientation.[24]

In 2003, Song et al.[25] revisited this problem using state of the art computer simulation studies to calculate, from first principles, thermodynamic properties (e.g., second virial coefficients) of methane/perfluoromethane mixtures. They employed the recently developed all atom optimized potentials for liquid simulations (OPLS-AA) potential energy model and used the geometric mean approximation to model interactions between alkanes and perfluoroalkanes. The objective was to determine whether the subtleties of molecular geometry and molecular charge distribution incorporated in the OPLS-AA potential would account for the apparent departure from the geometric mean approximation in calculating interaction energies between fluorocarbon and hydrocarbon molecules. Surprisingly, these refined models of molecular structure and electron distribution could not describe experimental data of second virial coefficients of mixing methane and perfluoromethane even though the models provided very accurate predictions of the thermodynamic properties of the pure components. The model calculations and experimental data could only be brought into concordance if the interaction energy between a methane molecule and a perfluoromethane molecule was reduced to a value 10% lower than that suggested by the geometric mean approximation.[25] Because mixture thermodynamic properties such as solubility depend exponentially on these interaction energies, small deviations in interaction energies yield large effects in observed properties. Finally, after trying many combinations of mixing rules and examining in detail the various contributions to the potential model, Song et al. concluded "At this point, it must be admitted that the origins of the weaker-than-expected interactions between perfluoroalkanes and alkanes remain a mystery."[25]

Interestingly, using an entirely different approach, based on modeling polymer−penetrant interactions using equations of state, De Angelis et al. observed that molecular interactions between hydrocarbon gases and fluoropolymers and between perfluorinated gases and hydrocarbon-based polymers are approximately 10% lower than predicted by the geometric mean rule.[26,27] As indicated above, properties such as sorption are quite sensitive to the unlike molecule interaction energy, so its reduction by 10% can cause large differences in solubility coefficients. For example, in the hydrocarbon polymer PDMS, the solubilities of fluorinated gases decrease by about 3−5-fold when the unlike molecule interaction energy is reduced by 10%.[26] Presumably, the fundamental scientific phenomenon that leads to the unexplained reduction in interaction energies between low molar mass hydrocarbons and fluorocarbons is also operative during gas sorption in polymers.

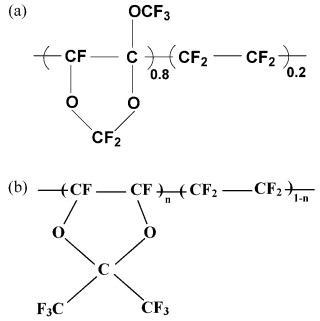

Figure 1. Chemical structure of (a) Hyflon AD 80 and (b) Teflon AF polymers. $n = 0.65$ for AF1600 and $n = 0.87$ for AF2400.

The high free volume fluoropolymers in Table 1 have rather low CO_2/CH_4 selectivities.[28,29] For example, at 35 °C and low to moderate pressures (up to 10 atm), the pure gas CO_2/CH_4 selectivities of AF1600 and AF2400 are 6.2 and 5.6, respectively.[28,29] A lower free volume glassy polymer would be expected to possess greater size-sieving ability and, therefore, greater CO_2/CH_4 selectivity. Also, gas molecules sorbing into a lower free volume matrix may find themselves, on average, in closer proximity to polymer chains in a dense polymer matrix and, therefore, experience stronger interactions with the surrounding polymer than they would in a high free volume material. Thus, it is of interest to study hydrocarbon solubility in a lower free volume fluoropolymer and compare it with that in higher free volume fluoropolymers and in hydrocarbon polymers. With these objectives in mind, we report gas solubility, permeability, and diffusivity of N_2, CO_2, and C1−C3 hydrocarbons as well as C_3F_8 solubility in a low free volume, glassy, amorphous copolymer composed of 80 mol % 2,2,4-trifluoro-5-trifluoromethoxy-1,3-dioxole (TTD) and 20 mol % tetrafluoroethylene (TFE), commercially known as Hyflon AD 80. The structure of Hyflon AD 80 is presented in Figure 1a.[30] This polymer has a glass transition temperature of 134 °C and a FFV of 0.197, which was estimated using Bondi's group contribution method and the reported density value of 1.918 g/cm^3.[31] Gas sorption and transport properties of this fluoropolymer are compared with those of a structurally similar family of high free volume fluoropolymers, called Teflon AF, that are depicted in Figure 1b. While permeabilities of H_2, N_2, O_2, CO_2, and CH_4 have been reported earlier for Hyflon AD 80,[32] we could not find reports of solubility or the pressure dependence of permeability or solubility in this polymer. Additionally, diffusion coefficients of gas molecules in this polymer have not been reported.

Background

Permeability. The permeability of a polymer film to a pure gas is given by[33]

$$P = \frac{Nl}{p_2 - p_1} \tag{1}$$

where P is the permeability coefficient, N is the steady-state gas flux through the polymer membrane, l is film thickness, p_2 is the feed or upstream pressure, and p_1 is the permeate or downstream pressure. Penetrant transport through a polymer film is commonly described by a three-step solution-diffusion mechanism.[33] According to this mechanism, when penetrant flux obeys Fick's law and the downstream pressure is negligible compared to the upstream pressure, the permeability coefficient, P can be expressed as[33]

$$P = SD \tag{2}$$

where D is the effective concentration-averaged diffusion coefficient. S, the solubility coefficient at the upstream pressure, is the ratio of the equilibrium concentration of the penetrant in the polymer at the upstream face of the membrane to the upstream pressure. The effective concentration-averaged diffusivity is defined by

$$D = \int_{C_1}^{C_2} \frac{D_{\text{loc}}}{1-\omega}\,\mathrm{d}C = \int_{C_1}^{C_2} D_{\text{eff}}\,\mathrm{d}C \tag{3}$$

where D_{loc} is the local concentration-dependent diffusion coefficient, ω is the penetrant mass fraction in the polymer at concentration C, and D_{eff} is the so-called local effective diffusion coefficient.

Selectivity. The ideal selectivity, $\alpha_{A/B}$, of component A over B is a measure of the potential separation characteristics of the membrane material. The ideal selectivity can be written as the ratio of the pure gas permeabilities:[33]

$$\alpha_{A/B} \equiv \frac{P_A}{P_B} \tag{4}$$

or

$$\alpha_{A/B} = \frac{S_A}{S_B}\frac{D_A}{D_B} \tag{5}$$

where the first term on the right-hand side of eq 5 is the solubility selectivity and the second is the diffusivity selectivity. In eqs 4 and 5, S_i, D_i, and P_i are the solubility, diffusivity, and permeability of gas i in the polymer, respectively.

Solubility. Sorption isotherms for gases in glassy polymers are usually concave to the pressure axis at low pressures and linear at higher pressures.[33] Such isotherms are often described using the dual mode sorption model.[34] In this model, penetrant molecules are viewed as being partitioned into two distinct populations, which are in dynamic equilibrium with each other: (i) penetrant molecules sorbed by a dissolution mechanism in the dense polymer matrix (Henry's law population) and (ii) penetrant molecules filling unrelaxed, molecular-scale gaps (microvoids) frozen into the glassy state (Langmuir population).[34] The dual mode model is expressed analytically as a sum of these two contributions to penetrant sorption:

$$C = k_D p + \frac{C'_H b p}{1 + bp} \tag{6}$$

where C is the total concentration of penetrant in the polymer, k_D is the Henry's law constant, C'_H is the hole saturation constant or Langmuir sorption capacity parameter, and b is the Langmuir affinity parameter.

Diffusivity. The local effective diffusion coefficient, D_{eff}, can be estimated from the slope of the sorption isotherm and the pressure dependence of permeability as follows:[35]

$$D_{\text{eff}}(C_2) = \left[P + \Delta p \frac{\mathrm{d}P}{\mathrm{d}\Delta p}\right]_{p_2}\left(\frac{\mathrm{d}p}{\mathrm{d}C}\right)_{p_2} \quad (7)$$

Experimental Section

Materials. Hyflon AD 80 was purchased from the Ausimont Co. (Thorofare, NJ), now Solvay Solexis. Uniform, isotropic films with thicknesses ranging from 35 to 90 μm were cast from 2% (w/v) solution (i.e., 2 g of polymer per 100 cm^3 of solvent) in PF 5060, a perfluorinated volatile solvent from 3M (St. Paul, MN). The films were dried at ambient conditions for 2−3 days and then utilized for sorption and permeation measurements. The pure gases and vapors used in the experiments had a purity of at least 99.5%. N_2, O_2, CO_2, CH_4, and C_2H_6 were obtained from National Specialty Gases (Durham, NC). C_3H_8 and C_3F_8 were purchased from Machine and Welding (Raleigh, NC). A gas mixture containing 20% CO_2 in CH_4 and another containing 10% CO_2, 50 ppm toluene, and 500 ppm *n*-hexane in CH_4 (primary standards with analyses provided) were purchased from MG Industries (Wilmington, DE) for the mixed-gas permeation experiments. All gases were used as received.

Sorption. Solubility coefficients were determined using a high-pressure barometric apparatus.[36] Initially, a polymer film was placed in the sample chamber and exposed to vacuum overnight to degas it. A known amount of penetrant gas was introduced into the chamber, and the pressure was allowed to equilibrate. Once the chamber pressure was constant, the amount of gas sorbed by the polymer was determined by performing a mass balance. Additional penetrant was introduced, and the procedure was repeated. In this incremental manner, penetrant uptake was determined as a function of pressure. The maximum pressure was 7−25 atm, depending on the penetrant. After measuring each isotherm, the polymer samples were degassed under vacuum overnight. The system temperature was controlled to ±0.1 °C using a constant temperature water bath. The sorption experiments were performed in the following order: N_2, CO_2, CH_4, C_2H_6, C_3H_8, and C_3F_8. A N_2 sorption experiment was also performed after each of the other penetrants to ensure that the polymer film had not undergone significant sorption hysteresis during the experiments. Isotherms for subsequent penetrants were measured only after the N_2 isotherm matched the initially measured isotherm.

Permeability. Pure gas permeability coefficients for N_2, O_2, and CO_2 were determined using a constant pressure/variable volume apparatus.[37] The membrane area was 13.8 cm^2. The upstream pressure was varied from 2.7 to 21.4 atm. The downstream pressure was atmospheric. Prior to each experiment, the upstream and downstream sides of the permeation cell were purged with penetrant gas. The system temperature was controlled to ±0.5 °C using a DYNA-SENSE temperature control system. Gas flow rates were measured with a soap-film bubble flowmeter. When steady-state conditions were attained, the following expression was used to evaluate permeability (cm^3 (STP) cm/(cm^2 s cmHg)):

$$P = \frac{22414}{A}\frac{l}{p_2 - p_1}\frac{p_1}{RT}\frac{\mathrm{d}V}{\mathrm{d}t} \quad (8)$$

where p_2 is the upstream pressure (cmHg), p_1 is the downstream pressure (atmospheric pressure in this case, i.e., 76 cmHg), l is the membrane thickness (cm), A is the membrane area (cm^2), T is the absolute temperature (K), R is the universal gas constant (6236.56 cm^3 cmHg/(mol K)), and dV/dt is the volumetric displacement rate of the soap film in the bubble flowmeter (cm^3/s).

Pure gas permeability coefficients of the hydrocarbons, CH_4, C_2H_6, and C_3H_8, were measured in a constant volume/variable pressure apparatus.[38] The membrane area was 13.8 cm^2. The upstream pressure was varied from 2.7 to 18 atm. The downstream side was maintained below 10 mmHg. Prior to each experiment, the upstream and downstream sides of the permeation cell were evacuated to below 0.5 mmHg. The system temperature was controlled to ±0.5 °C using an Omega CN76000 temperature controller. The increase in pressure on the downstream side was recorded using a data acquisition system employing Labtech software. When the rate of pressure increase on the downstream side, dp/dt (cmHg/s), attained its pseudo-steady-state value, the permeability (cm^3 (STP) cm/(cm^2 s cmHg)) was calculated using the expression

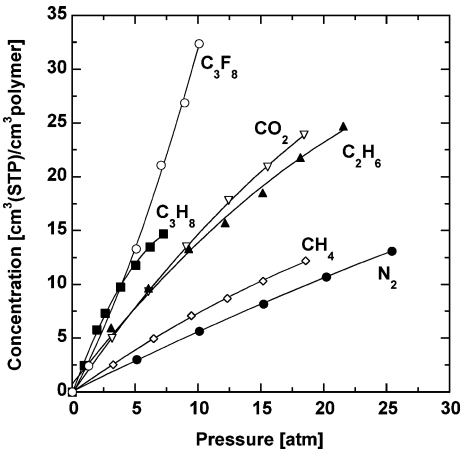

Figure 2. Sorption isotherms of N_2, CO_2, C1−C3 hydrocarbons, and C_3F_8 in Hyflon AD 80 at 35 °C.

$$P = \frac{22414}{A}\frac{l}{p_{\text{abs}}}\frac{V}{RT}\frac{\mathrm{d}p}{\mathrm{d}t} \quad (9)$$

where p_{abs} is the upstream pressure (cmHg) and V is the downstream volume (cm^3).

Mixed Gas Permeability. Mixed gas CO_2 and CH_4 permeabilities and CO_2/CH_4 selectivity of Hyflon AD 80 were measured in a constant volume/variable pressure permeation apparatus similar to the one described by O'Brien et al.[39] A 4.7 cm diameter polymer sample disk was placed in a permeation cell (Millipore) modified for gas permeation measurements. The film was masked with Al foil, exposing an area of 3.9 cm^2 for gas permeation. The cell was placed in an oven heated to 35 °C. The cell provided ports for a feed stream and a retentate stream on the upstream side of the sample film and for a permeate stream on the downstream side of the film. The CO_2−CH_4 feed pressure was 8−53.2 atm, while for the hydrocarbon-containing feed, it was set at 35 atm. The retentate flow rate was set to a sufficiently high value to ensure that the maximum stage cut was less than 1%. The permeate pressure was maintained below 9 mmHg. The increase in pressure on the downstream side of the film was recorded using a data acquisition system employing Labview software. When the rate of pressure increase on the downstream side attained its pseudo-steady-state value, the permeability of each gas was calculated using the expression

$$P_{\text{A}} = \frac{22414}{A}\frac{l}{x_{\text{A}}p_{\text{abs}}}\frac{V}{RT}y_{\text{A}}\frac{\mathrm{d}p}{\mathrm{d}t} \quad (10)$$

where P_{A} is the permeability of gas A (cm^3 (STP) cm/(cm^2 s cmHg)), x_{A} and y_{A} are the mole fractions of A in the feed and permeate streams, respectively, p_{abs} is the total upstream pressure (cmHg), and dp/dt is the steady rate of total pressure increase with time in the downstream volume (cmHg/s). The compositions of the feed and permeate streams were measured by a HP 5890 gas chromatograph with a thermal conductivity detector and high-purity He as carrier gas. The mixed-gas CO_2/CH_4 selectivity was the ratio of the two gas permeabilities calculated using eq 10.

Results and Discussion

Solubility. Figure 2 presents gas sorption isotherms in Hyflon AD 80 at 35 °C. Except for C_3F_8, which is the most soluble penetrant at high pressures, all isotherms

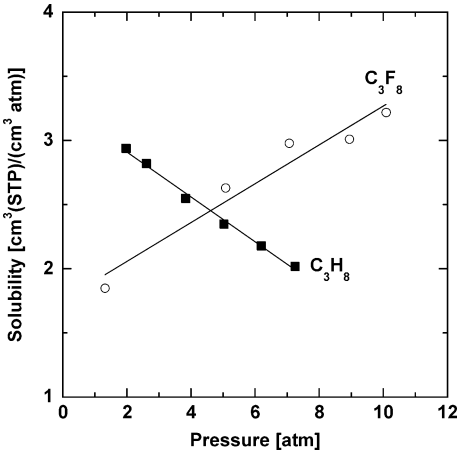

Figure 3. Comparison of C_3H_8 (■) and C_3F_8 (○) solubility in Hyflon AD 80 at 35 °C as a function of pressure. These data were calculated using data in Figure 2 and the definition of solubility as the ratio of the equilibrium concentration of the penetrant in the polymer at the upstream face of the membrane to the upstream pressure.

are concave to the pressure axis, which is characteristic of gas sorption in glassy polymers at low to moderate pressures.[33] The infinite dilution solubilities of these gases increase in the order

$$N_2 < CH_4 < CO_2 \approx C_2H_6 < C_3F_8 < C_3H_8$$

This is also the order of increasing gas critical temperature and, hence, gas condensability. C_3F_8 solubility, while lower than that of C_3H_8 at very low pressures, rises above that of C_3H_8 at higher pressures (cf. Figure 3). At low pressures, sorption in a glassy polymer occurs preferentially in the frozen microvoids that constitute the nonequilibrium excess free volume of glassy polymers.[34] Molecules sorbing into these preexisting microvoids at low pressure experience weaker interactions with the polymer matrix than those sorbing into more dense regions of the polymer where a gap must be created to accommodate the penetrant. Therefore, sorption at low pressures is likely to be strongly influenced by penetrant condensability and weakly influenced by interactions with the glassy polymer. This hypothesis is consistent with higher sorption of C_3H_8 at lower pressures. At higher pressures, interactions with the polymer have a more pronounced effect on solubility as penetrant molecules sorb increasingly into more densified regions of the polymer. Because of its chemical similarity with the polymer, C_3F_8 enjoys more favorable interactions with this fluoropolymer than does C_3H_8, and this better chemical affinity for the polymer is consistent with C_3F_8 solubility exceeding that of C_3H_8 at higher pressures.

The ratio of C_3H_8 to N_2 solubility in Hyflon AD 80 at infinite dilution conditions is approximately 6, which is 2.5−3.5 times lower than in the high free volume, glassy fluoropolymers, AF1600 and AF2400, and about 16 times lower than that in polyethylene (cf. Table 1). Thus, the lower free volume glassy fluoropolymer displays much lower sorption for hydrocarbon penetrants, such as C_3H_8, relative to N_2, than higher free volume fluoropolymers or hydrocarbon polymers. While the influence of differences in chemical structure among the fluoropolymers on solubility cannot be ruled out, it is interesting that C_3H_8/N_2 solubility ratio decreases systematically as fractional free volume decreases (cf. Table 1). Also, with increasing penetrant pressure, the C_3H_8/N_2 solubility ratio decreases for each fluoropolymer as penetrants sorb to a greater extent into the densified regions of the polymer (cf. Figure 4). The high free volume AF materials, which have large Langmuir microvoid capacities, exhibit a more significant decrease than that of the lower free volume Hyflon AD 80.

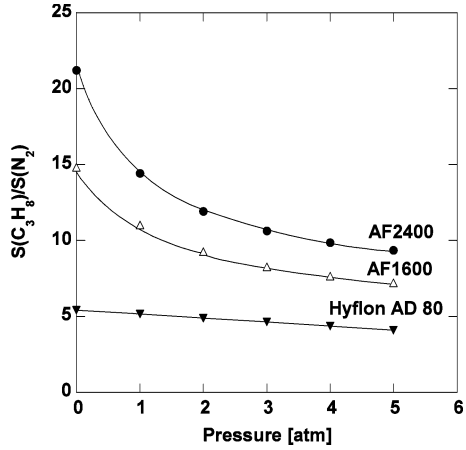

Figure 4. Variation of C_3H_8/N_2 solubility ratio with pressure for Teflon AF polymers[28] and Hyflon AD 80 at 35 °C.

Table 2. Slope of the Correlation of the Natural Logarithm of Solubility vs Penetrant Critical Temperature for Hydrocarbons and Fluorocarbons at 35 °C

classification	medium	$b \times 10^3$ (K^{-1})
hydrocarbons	benzene[46]	17[a]
	n-heptane[46]	18[a]
	natural rubber[16]	18[a]
	amorphous polyethylene[16]	16[a]
	poly(butadiene)-hydrogenated[16]	17[a]
	poly(dimethylsiloxane)[17]	17[b]
	polysulfone[42]	17[c]
	poly(phenylene oxide)[40]	16[d]
	poly(ethylene terephthalate)[54]	19[e]
fluorocarbons	*n*-C_7F_{16}[46]	10.5[a]
	AF1600[28]	11[f]
	Hyflon AD 80	7 ± 0.3

[a] 25 °C and 1 atm. [b] 35 °C [c] 35 °C and 10 atm for all gases except *n*-C_4H_{10} which is at infinite dilution. [d] 35 °C and infinite dilution. [e] 24−45 °C and infinite dilution. [f] Based on solubility data at 25 °C.

As mentioned earlier, the natural logarithm of gas solubility in polymers often increases linearly with an increase in gas critical temperature, normal boiling point, or Lennard-Jones force constant.[15] Interestingly, the best fit linear correlations have similar slopes for hydrocarbon gas and vapor solubility in a large number of hydrocarbon-based polymers and liquids.[40] For example, if gas critical temperature is used as a measure of condensability, the best fit slopes for many hydrocarbon rubbery polymers, glassy polymers, and liquids lie in a narrow range around 0.019 K^{-1} when gas solubility is measured at 35 °C (cf. Table 2). This slope value had been predicted on the basis of simple thermodynamic considerations by Gee.[41] Figure 5 shows the correlation between gas solubility and penetrant critical temperature in Hyflon AD 80 at infinite dilution conditions and compares it with data for a typical hydrocarbon-based membrane polymer, polysulfone.[42] The figure also displays infinite dilution gas solubility data in AF1600.[28]

From Figure 5, permanent gases such as N_2 and O_2 appear to exhibit higher sorption in the two fluoropoly-

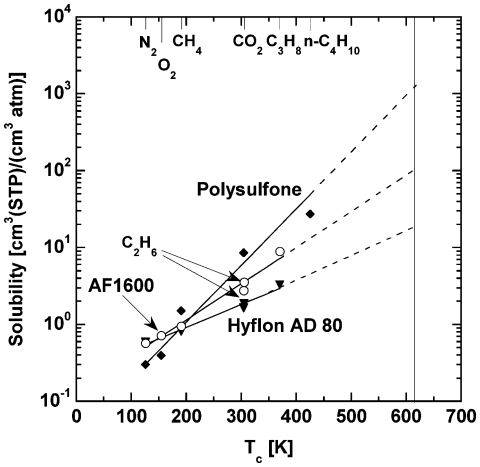

Figure 5. Correlation between gas solubility and critical temperature in polysulfone,[42] AF1600,[28] and Hyflon AD 80 at 35 °C. Polysulfone data are at 10 atm except for *n*-C_4H_{10} which is at infinite dilution, as are the data for the other two polymers. The vertical line at a T_c value of 617.7 K corresponds to the critical temperature of *n*-decane.

mers than in polysulfone. Permanent gas solubility is often higher in fluorinated media than in their hydrocarbon analogues,[23] and fluorinated liquids have been considered as additives to increase the oxygen solubility of blood substitutes, in part, because of their high O_2 sorption capacity.[43] This higher sorption capacity for permanent gases in fluorinated liquids is thought to be predominantly due to the structure of the fluid, with attractive intermolecular forces playing a minor role.[44] Fluorine atoms attached to the carbon backbone of fluorocarbons are larger than the hydrogen atoms on analogous hydrocarbon chains. It is hypothesized that the larger fluorine atoms influence the molecular scale packing in fluorocarbons in such a way that more large-sized cavities are formed in fluorocarbon liquids than in hydrocarbon liquids.[44] These larger cavities enhance the ability of the fluorocarbon liquid to dissolve significant quantities of gases.[44] This hypothesis also explains the lower boiling points and higher viscosities of fluorinated compounds.[43] Also, perfluorinated liquids have lower cohesive energy densities (CED) than their hydrocarbon analogues. For example, the CED of perfluoro-*n*-heptane (*n*-C_7F_{16}) is 36.25 cal/cm^3 as compared to 55.3 cal/cm^3 for *n*-heptane.[45] Similarly, the CED values for perfluorobenzene and benzene are 68.5 and 83.7 cal/cm^3, respectively.[45] Lower cohesive energy density also contributes to increased gas sorption.[33] It is not unreasonable to expect the existence of these effects in fluoropolymers. Thus, higher nitrogen solubility in fluoropolymers is expected to be primarily due to polymer properties like free volume distribution and low CED than due to any specific interactions with the permanent gases.

Following the above reasoning, the solubility of larger penetrants such as hydrocarbons should also be correspondingly higher in fluoropolymers. However, as noted above, the solubility ratio of propane to that of nitrogen is much less in perfluorinated media due to specific interactions between hydrocarbons and fluorocarbons which suppress hydrocarbon solubility in these materials. In fact, the solubility of larger, more condensable hydrocarbon gases increases less rapidly with increasing critical temperature in fluoropolymers than in hydrocarbon polymers. That is, the slope of the best

Table 3. Slope of the Correlation of the Natural Logarithm of Solubility vs Penetrant Critical Temperature in the Teflon AF Materials[28] and in Hyflon AD 80 at 35 °C

	slope, $b \times 10^3$ (K^{-1})	
polymer	$p = 0$ atm	$p = 5$ atm
AF2400	12.5	9
AF1600	11	8
Hyflon AD 80	7 ± 0.3	6 ± 0.3

fit trendline of the natural logarithm of solubility vs critical temperature is much lower in fluoropolymers than in hydrocarbon-based materials (cf. Table 2). From Table 2, polysulfone has a best fit slope value of 0.017 K^{-1}, which is similar to that of most hydrocarbon polymers.[7] AF1600 has a significantly lower slope of 0.011 K^{-1} despite having a much higher fractional free volume than polysulfone. Hyflon AD 80 has an even lower slope of 0.007 K^{-1} ($\pm$0.0003 K^{-1}). Liquid perfluoro-*n*-heptane (*n*-C_7F_{16}) has a slope of 0.0105 K^{-1}.[46]

The lower slope for Hyflon AD 80 at infinite dilution indicates a greater suppression of hydrocarbon solubility in this fluoropolymer than in AF1600. As mentioned earlier, gas solubility in glassy polymers at very low pressures is assumed to occur primarily in Langmuir microvoids frozen into the polymer matrix due to the nonequilibrium nature of the polymer. Sorption in these preexisting gaps depends strongly on penetrant condensability, which is constant for a given penetrant at fixed temperature and pressure. In such cases, infinite dilution solubility of a penetrant in different polymers should be influenced, primarily, by differences in available nonequilibrium free volume for sorption and interactions between the penetrant and the polymer chains. These fluoropolymers, while structurally quite similar, do have chemical structure differences that might contribute to differences in penetrant solubility, and systematic material sets are not available to definitively decouple free volume effects from chemical structure effects. However, from Tables 2 and 3, the systematic change in slope with fluoropolymer fractional free volume is intriguing, and it raises the possibility of a significant effect of available nonequilibrium excess free volume on the infinite dilution solubility. At higher pressures, sorption occurs in the denser, less energetically accessible regions of the polymer matrix, where penetrant molecules and polymer segments are expected to be closer, and greater solubility suppression might be observed at these pressures than at infinite dilution. From Table 3, the slopes of the solubility correlation for Teflon AF at 5 atm are lower than at infinite dilution, which is consistent with the above reasoning. The decrease in slope is more pronounced for higher free volume polymers due to their larger Langmuir sorption capacity. For Hyflon AD 80, the slope value at high pressure is very close to that at infinite dilution.

If the trend lines in Figure 5 are extrapolated beyond the range of presently available experimental data, a large hydrocarbon like *n*-decane ($T_c = 617.7$ K)[2] would have approximately 6 times lower solubility in AF1600 than in polysulfone. Also, Hyflon AD 80 is estimated to sorb about 60 times less *n*-decane than polysulfone and about 10 times less than AF1600. Because of inherently low solubility for such large hydrocarbons, low free volume fluoropolymers may be more resistant to plasticization caused by sorption of these compounds into the polymer matrix. However, more experimental mixed gas permeation studies of a variety of fluoropolymers

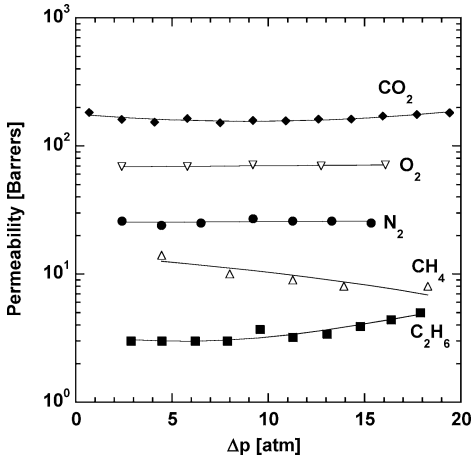

Figure 6. Permeability of N_2, O_2, CO_2, CH_4, and C_2H_6 in Hyflon AD 80 at 35 °C as a function of pressure difference across the membrane.

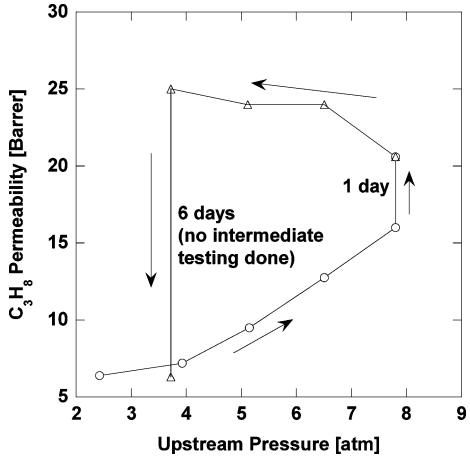

Figure 7. C_3H_8 permeability with increasing (○) and decreasing (Δ) pressure in Hyflon AD 80 at 35 °C. Arrows indicate the order of testing.

are required to understand the full extent to which this hypothesis might be valid.

Permeability. Figure 6 displays the permeability of Hyflon AD 80 to N_2, O_2, CO_2, CH_4, and C_2H_6 as a function of pressure difference across the membrane up to 20 atm at 35 °C. The penetrant permeabilities decrease as size increases:

$$CO_2 > O_2 > N_2 > CH_4 > C_2H_6$$

These permeability coefficients, measured in dense films, are 2−3 times lower than those reported by Arcella et al. in a composite membrane of this polymer on a PVDF support.[32] The source of this discrepancy is not known, although it can be challenging to measure the effective thickness in a composite membrane, and the influence of substructure resistance in Arcella et al.'s data was not reported.[32] From Figure 6, the permeabilities of N_2 and O_2 are independent of pressure while CH_4 permeability decreases with increasing pressure. In contrast, the permeabilities of CO_2 and C_2H_6 increase somewhat at higher pressures. Permanent gases and low-condensability penetrants typically exhibit constant or decreasing permeabilities with increasing penetrant pressure in glassy polymers due to the dual modes of sorption and transport available in these materials.[33] Also, at high gas pressures or penetrant activities, penetrants can plasticize the polymer matrix, which increases their permeabilities at higher pressures.[33]

C_3H_8 permeability in Hyflon AD 80 is presented in Figure 7. Multiple measurements were made at each pressure over a period of 1−2 days before increasing the upstream pressure. At the highest pressure, a considerable difference in permeability was measured on successive days, as shown in the figure. Then, the upstream pressure was decreased, and measurements were made in a similar fashion. After measuring permeability at the lowest pressure, the polymer film was left in the permeation cell for 6 days before the final measurement was made. The polymer exhibits considerably higher permeability values in the decreasing-pressure cycle than that measured in the increasing-pressure cycle. This hysteresis effect is a likely result of alterations in the glassy polymer matrix due to exposure to high activity penetrants and has been previously observed in other glassy polymers.[47,48] During the increasing-pressure cycle, the penetrant causes subtle perturbations in chain-packing conformations and also increases

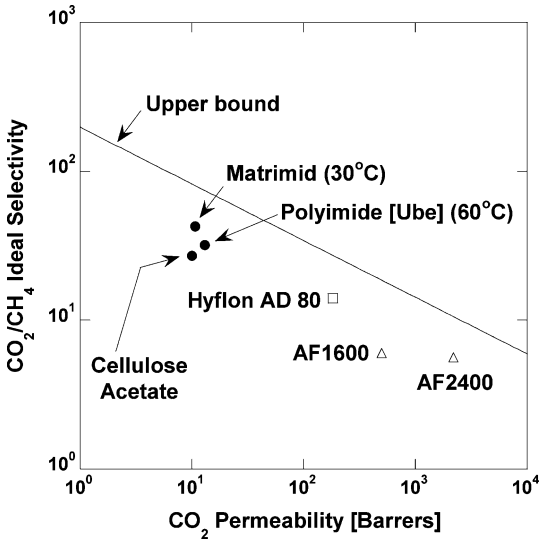

Figure 8. Comparison of CO_2/CH_4 separation performance of Hyflon AD 80 (□) based on pure gas permeabilities with select hydrocarbon polymers (●)[4] and high free volume fluoropolymers (△).[28,29] Temperature = 35 °C, unless mentioned otherwise.

packing defect size in the matrix.[47] These alterations persist in glassy polymers due to low mobility of polymer chain segments below their glass transition temperature. As seen from Figure 7, in this specific example, the polymer returns to its original permeability within 6 days, which is a relatively short duration compared to previous reports in other glassy, hydrocarbon-based polymers.[47,48]

Figure 8 compares the CO_2/CH_4 separation performance, based on pure gas permeation experiments, of Hyflon AD 80 at 35 °C and 4.4 atm upstream pressure with three hydrocarbon-based polymers with attractive separation properties for CO_2 removal from natural gas.[4] The figure also shows the separation performance of two high free volume fluoropolymers, AF2400 and AF1600. The upper bound line denotes the best properties achieved to date by polymers considered for this separation.[49] Hyflon AD 80 is approximately 1 order of magnitude more permeable to CO_2 than the hydrocarbon-based polymers, but its CO_2/CH_4 selectivity is 2−3 times lower. However, Hyflon AD 80 lies approximately the same distance from the upper bound line as the hydro-

Table 4. Mixed Gas Performance of Hyflon AD 80 at 35 °C When Exposed to a Feed Stream of 20% CO_2 in CH_4

total feed pressure (atm)	CO_2 permeability (barrers)	CO_2/CH_4 selectivity
8.2	257	10.6
14.3	266	10.3
21.0	286	10.2
35.0	276	9.3
53.2	281	8.7

carbon polymers, so it appears to be an encouraging start for this materials design concept.

Systematic structure−property studies have shown that polymers with greater chain rigidity and sufficient chain spacing have better combinations of permeability and selectivity for gas separations.[3] Polymers meeting these requirements usually have significant aromatic character and bulky groups on the chain.[50,51] In this respect, the structure of Hyflon AD 80 more closely resembles that of aliphatic polymers that do not have attractive gas separation properties. This observation suggests a potential opportunity to considerably improve the materials performance of fluorinated polymers via systematic structure−property studies.

Mixed-Gas Permeability. CO_2−CH_4 mixed-gas permeation properties of Hyflon AD 80 were determined using a feed gas mixture containing 20% CO_2 in CH_4 at 35 °C and 8−53.2 atm total pressure. The separation performance of the film is recorded in Table 4. The film exhibited a CO_2 permeability of approximately 250 barrers and a CO_2/CH_4 mixture selectivity of 10.6 at 8.2 atm feed pressure. Upon increasing pressure to 53.2 atm, the CO_2 permeability increased slightly to 280 barrers, while the mixed gas CO_2/CH_4 selectivity decreased slightly to 8.7. Thus, this material exhibits a minor decrease in selectivity at CO_2 partial pressures up to 10.6 atm. This result is in striking contrast to the dramatic decrease in selectivity with increasing CO_2 partial pressure in the high-performance hydrocarbon-based polyimide materials discussed in the Introduction.[8,9] From Figure 2, CO_2 concentration in Hyflon AD 80 is only about 15 cm^3 (STP)/cm^3 at 10 atm. CO_2 concentration in the 6FDA polyimide family is reported to be much higher.[51,52] While we could not find CO_2 concentrations in the 6FDA polyimides mentioned in the Introduction, the reported CO_2 concentrations in other 6FDA polyimides are in excess of 30 cm^3 (STP)/cm^3 at 10 atm.[51,52] This difference in CO_2 solubilities between the fluoropolymer and the polyimides is consistent with the greater CO_2-induced plasticization resistance of Hyflon AD 80.

The polymer film was also exposed to a feed stream containing 10% CO_2, 50 ppm toluene, and 500 ppm *n*-hexane in CH_4 at 35 °C and 35 atm total pressure. This gas stream has a dew point in the range of −29 to −40 °C, depending on the equation of state used to estimate the dew point. In comparison, natural gas at field conditions has a dew point of −20 °C when it is fed to a membrane module for CO_2 removal. Thus, the gas mixture has a comparable but somewhat lower dew point to that experienced in industrial environments. When exposed to this gas mixture, the polymer exhibited a CO_2 permeability of about 270 barrers and a CO_2/CH_4 selectivity of 10.6 after 3 h. These values remained constant after 22 h of exposure to this feed mixture. Thus, the polymer exhibited undetectable hydrocarbon-induced plasticization in the presence of moderate concentrations of model higher hydrocarbons in the feed stream.

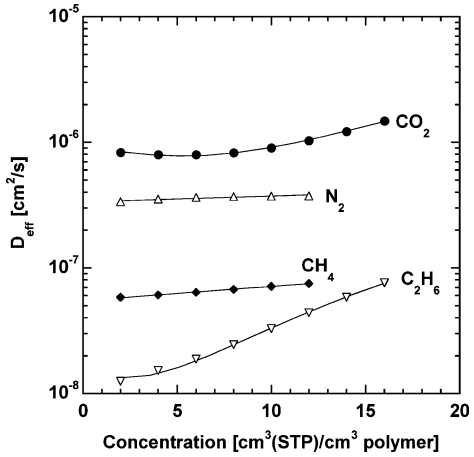

Figure 9. Effective diffusion coefficients of N_2, CO_2, CH_4, and C_2H_6 in Hyflon AD 80 as a function of upstream penetrant concentration in the polymer at 35 °C.

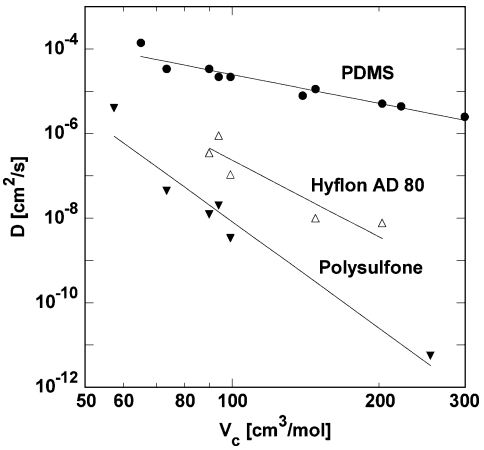

Figure 10. Comparison of the variation of infinite dilution diffusion coefficients with penetrant critical volume in Hyflon AD 80 with that in a typical rubbery (PDMS) and glassy (polysulfone) polymer. The trendlines in the figure satisfy the equation $D = \tau V_c^{-\eta}$, where η is a measure of the size sieving ability or size selectivity of the polymer to penetrants. The best-fit values of η in the plot are the following: PDMS, 2.3; polysulfone, 8.4; Hyflon AD 80, 6.0 ± 0.6.

Diffusivity. Effective diffusion coefficients of N_2, CO_2, CH_4, and C_2H_6 as a function of pressure in Hyflon AD 80 are presented in Figure 9. The values were calculated using eq 7. From the figure, the diffusivities of N_2 and CH_4 are independent of penetrant concentration in the polymer. D_{eff} for the more condensable gases, CO_2 and C_2H_6, increases with penetrant concentration at higher pressures, indicating plasticization. The diffusion coefficients decrease with increasing penetrant size, in agreement with the trend in permeability coefficients. The variation of diffusion coefficients with critical volume (a measure of penetrant size) is usually described by the equation

$$D = \frac{\tau}{V_c^{\eta}} \tag{11}$$

where τ and η are adjustable parameters. η provides a measure of the rate of decrease of diffusion coefficients with increasing penetrant size; the higher the value of η, the greater the diffusivity selectivity of the polymer. Figure 10 compares the diffusivity selectivity or "size-sieving" ability of Hyflon AD 80 with that of a typical

rubbery (PDMS) and glassy (polysulfone) polymer. The glassy polymer, polysulfone, exhibits a greater decrease in the diffusion coefficient with increase in penetrant size than rubbery PDMS; it has an η value of 8.4 compared to only 2.3 for PDMS. Thus, the glassy polymer is able to separate molecules better on the basis of their size differences. Hyflon AD 80 has an η value of approximately 6, thus exhibiting a much stronger size-sieving ability than rubbery PDMS but slightly lower than the aromatic, glassy polymer, polysulfone. As mentioned before, high-performance polymers for this application usually have very strong size-sieving abilities and significant aromatic character. Thus, designing fluoropolymers with greater size-sieving abilities might lead to better separation performance membranes for CO_2 removal from natural gas.

Conclusions

Hyflon AD 80 exhibits a much lower slope in the correlation of natural logarithm of hydrocarbon solubility and penetrant critical temperature than hydrocarbon-based polymers and even high free volume fluoropolymers like AF1600. Thus, this polymer may have inherently lower solubility for large hydrocarbon compounds than hydrocarbon polymers and, therefore, may exhibit greater resistance to plasticization by these compounds than conventional hydrocarbon-based membrane polymers. Permanent gas and light hydrocarbon permeabilities in this polymer decrease with increasing penetrant size, following the same trend as the diffusion coefficients. In CO_2-CH_4 mixed-gas permeation experiments where the feed gas partial pressure of CO_2 was as high as 10.6 atm, the polymer exhibits relatively little CO_2-induced plasticization. The polymer also showed excellent plasticization resistance to moderate concentrations of toluene and *n*-hexane in the CO_2-CH_4 gas stream. There is some evidence of plasticization of this polymer by pure CO_2 and C_2H_6 at higher pressures, based on the increase in diffusion coefficients with concentration. The polymer exhibits significant hysteresis of C_3H_8 permeability, indicating long-lived disturbances of the polymer matrix upon exposure to high-activity propane.

Acknowledgment. The authors gratefully acknowledge partial support of this work by the Chemical Sciences, Geosciences and Biosciences Division, Office of Basic Energy Sciences, Office of Science, U.S. Department of Energy (DE-FG03-02ER15362).

References and Notes

(1) Spillman, R. W. Economics of Gas Separation Membranes. *Chem. Eng. Prog.* **1989**, 41−62.
(2) Reid, R. C.; Prausnitz, J. M.; Poling, B. E. *The Properties of Gases and Liquids*, 4th ed.; McGraw-Hill: New York, 1987.
(3) Koros, W. J.; Hellums, M. W. *Fluid Phase Equilib.* **1989**, *53*, 339−354.
(4) Baker, R. W. *Membrane Technology and Applications*; McGraw-Hill: New York, 2000.
(5) Ratcliffe, C. T.; Diaz, A.; Nopasit, C.; Munoz, G. Application of Membranes in CO_2 Separation from Natural Gas: Pilot Plant Tests on Offshore Platforms. Paper presented at the Laurence Reid Gas Conditioning Conference, Norman, OK, 1999.
(6) Brandrup, J.; Immergut, E. H.; Grulke, E. A. *Polymer Handbook*, 4th ed.; Wiley-Interscience: New York, 1999.
(7) Prabhakar, R. S.; Freeman, B. D. In *Advanced Materials for Membrane Separations*; Pinnau, I., Freeman, B. D., Eds.; American Chemical Society: Washington, DC, 2004; Vol. 876, pp 106−128.
(8) Staudt-Bickel, C.; Koros, W. J. *J. Membr. Sci.* **1999**, *155*, 145−154.
(9) White, L. S.; Blinka, T. A.; Kloczewski, H. A.; Wang, I.-F. *J. Membr. Sci.* **1995**, *103*, 73−82.
(10) Bos, A.; Punt, I. G. M.; Wessling, M.; Strathmann, H. *J. Polym. Sci., Part B: Polym. Phys.* **1998**, *36*, 1547−1556.
(11) Bos, A.; Punt, I.; Strathmann, H.; Wessling, M. *AIChE J.* **2001**, *47*, 1088−1093.
(12) Bos, A.; Punt, I. G. M.; Wessling, M.; Strathmann, H. *Sep. Purif. Technol.* **1998**, *14*, 27−39.
(13) Wind, J. D.; Staudt-Bickel, C.; Paul, D. R.; Koros, W. J. *Ind. Eng. Chem. Res.* **2002**, *41*, 6139−6148.
(14) Wind, J. D.; Staudt-Bickel, C.; Paul, D. R.; Koros, W. J. *Macromolecules* **2003**, *36*, 1882−1888.
(15) Freeman, B. D.; Pinnau, I. In *Polymer Membranes for Gas and Vapor Separation*; Freeman, B. D., Pinnau, I., Eds.; American Chemical Society: Washington, DC, 1999; Vol. 733, pp 1−27.
(16) Michaels, A. S.; Bixler, H. J. *J. Polym. Sci.* **1961**, *50*, 393−412.
(17) Kamiya, Y.; Naito, Y.; Terada, K.; Mizoguchi, K. *Macromolecules* **2000**, *33*, 3111−3119.
(18) Merkel, T. C.; Bondar, V.; Nagai, K.; Freeman, B. D. *Macromolecules* **1999**, *32*, 370−374.
(19) Merkel, T. C.; Bondar, V. I.; Nagai, K.; Freeman, B. D.; Pinnau, I. *J. Polym. Sci., Part B: Polym. Phys.* **2000**, *38*, 415−434.
(20) Pinnau, I.; He, Z.; Da Costa, A. R.; Amo, K. D.; Daniels, R. US Patent 6,361,582 B1, 2002.
(21) Pinnau, I.; He, Z.; Da Costa, A. R.; Amo, K. D.; Daniels, R. US Patent 6,361,583 B1, 2002.
(22) Hildebrand, J. H.; Prausnitz, J. M.; Scott, R. L. *Regular and Related Solutions*; Van Nostrand Reinhold Co.: New York, 1970.
(23) Wilhelm, E.; Battino, R. *J. Chem. Thermodyn.* **1971**, *3*, 761−768.
(24) Scott, R. L. *J. Phys. Chem.* **1958**, *62*, 136−145.
(25) Song, W.; Rossky, P. J.; Maroncelli, M. *J. Chem. Phys.* **2003**, *119*, 9145−9162.
(26) De Angelis, M.-G.; Merkel, T. C.; Bondar, V. I.; Freeman, B. D.; Doghieri, F.; Sarti, G. C. *J. Polym. Sci., Part B: Polym. Phys.* **1999**, *37*, 3011−3026.
(27) De Angelis, M.-G.; Merkel, T. C.; Bondar, V. I.; Freeman, B. D.; Doghieri, F.; Sarti, G. C. *Macromolecules* **2002**, *35*, 1276−1288.
(28) Alentiev, A. Y.; Shantarovich, V. P.; Merkel, T. C.; Bondar, V. I.; Freeman, B. D.; Yampolskii, Y. P. *Macromolecules* **2002**, *35*, 9513−9522.
(29) Merkel, T. C.; Bondar, V.; Nagai, K.; Freeman, B. D.; Yampolskii, Y. P. *Macromolecules* **1999**, *32*, 8427−8440.
(30) Arcella, V.; Ghielmi, A.; Tommasi, G. *Ann. N.Y. Acad. Sci.* **2003**, *984*, 226−244.
(31) Bondi, A. *Physical Properties of Molecular Crystals, Liquids and Glasses*; Wiley: New York, 1968.
(32) Arcella, V.; Colaianna, P.; Maccone, P.; Sanguineti, A.; Gordano, A.; Clarizia, G.; Drioli, E. *J. Membr. Sci.* **1999**, *163*, 203−209.
(33) Ghosal, K.; Freeman, B. D. *Polym. Adv. Technol.* **1993**, *5*, 673−697.
(34) Barrer, R. M.; Barrie, J. A.; Slater, J. *J. Polym. Sci.* **1958**, *27*, 177−197.
(35) Stern, S. A.; Shah, V. M.; Hardy, B. J. *J. Polym. Sci., Part B: Polym. Phys.* **1987**, *25*, 1263−1298.
(36) Bondar, V. I.; Freeman, B. D.; Pinnau, I. *J. Polym. Sci., Part B: Polym. Phys.* **1999**, *37*, 2463−2475.
(37) Stern, S. A.; Gareis, P. J.; Sinclair, T. F.; Mohr, P. H. *J. Appl. Polym. Sci.* **1963**, *7*, 2035−2051.
(38) Felder, R. M.; Huvard, G. S. In *Methods of Experimental Physics*; Fava, R. A., Ed.; Academic Press: New York, 1980; Vol. 16, Part C, pp 315−377.
(39) O'Brien, K. C.; Koros, W. J.; Barbari, T. A. *J. Membr. Sci.* **1986**, *29*, 229−238.
(40) Toi, K.; Morel, G.; Paul, D. R. *J. Appl. Polym. Sci.* **1982**, *27*, 2997−3005.
(41) Gee, G. *Q. Rev. (London)* **1947**, *1*, 265−298.
(42) Ghosal, K.; Chern, R. Y.; Freeman, B. D.; Savariar, R. *J. Polym. Sci., Part B: Polym. Phys.* **1995**, *33*, 657−666.
(43) Wesseler, E. P.; Iltis, R.; Clark, L. C., Jr. *J. Fluorine Chem.* **1977**, *9*, 137−146.
(44) Hamza, M. H. A.; Serratrice, G.; Stebe, M.-J.; Delpuech, J.-J. *J. Magn. Reson.* **1981**, *42*, 227−241.

(45) DIPPR Chemical Database, Thermophysical Properties Laboratory, Brigham Young University, Provo, UT; available at http://dippr.byu.edu/public/chemsearch.asp.
(46) Jolley, J. E.; Hildebrand, J. H. *J. Am. Chem. Soc.* **1958**, *80*, 1050−1054.
(47) Jordan, S. M.; Koros, W. J.; Fleming, G. K. *J. Membr. Sci.* **1987**, *30*, 191−212.
(48) Jordan, S. M.; Fleming, G. K.; Koros, W. J. *J. Polym. Sci., Part B: Polym. Phys.* **1990**, *28*, 2305−2327.
(49) Robeson, L. M. *J. Membr. Sci.* **1991**, *62*, 165−185.
(50) Koros, W. J.; Fleming, G. K. *J. Membr. Sci.* **1993**, *83*, 1−80.
(51) Stern, S. A. *J. Membr. Sci.* **1994**, *94*, 1−65.
(52) Coleman, M. R.; Koros, W. J. *J. Membr. Sci.* **1990**, *50*, 285−297.
(53) Merkel, T. C.; Bondar, V.; Nagai, K.; Freeman, B. D. *J. Polym. Sci., Part B: Polym. Phys.* **2000**, *38*, 273−296.
(54) Serad, G. E.; Freeman, B. D.; Stewart, M. E.; Hill, A. J. *Polymer* **2001**, *42*, 6929−6943.

MA048909F